Biomedical Signal Processing and Control 60 (2020) 101942

Contents lists available at ScienceDirect

Biomedical Signal Processing and Control

journal homepage: www.elsevier.com/locate/bspc

Investigation on the effect of Womersley number, ECG and PPG features for cuff less blood pressure estimation using machine learning

Geerthy Thambiraj, Uma Gandhi*, Umapathy Mangalanathan, V. Jeya Maria Jose, M. Anand

Department of Instrumentation and Control Engineering, National Institute of Technology, Tiruchirappalli, India

ARTICLE INFO

Article history:
Received 23 October 2019
Received in revised form 13 February 2020
Accepted 28 March 2020
Available online 7 May 2020

Keywords:
Continuous cuffless blood pressure
Random forest
Womersley parameter
ECG features
Genetic algorithm

ABSTRACT

Objective: Regulation and inhibition of high blood pressure, known as hypertension are intricate, and it demands a continuous, accurate blood pressure measurement system. All the existing continuous non-invasive techniques own challenges such as exact placement of the sensor, reconstruction of arterial pressure from finger cuff, frequent and subject based calibration. This paper presents an algorithm based on new time-domain features for continuous blood pressure monitoring which is crucial in intensive care units and can be used to predict cardiovascular ailments.
Methods: Here, we propose the method to estimate BP that extracts informative features like Womersley number (α), QRS, QTc interval, SDI from ECG and PPG signals and regression techniques which are employed to estimate blood pressure continuously. Performance metrics like MAE, RMSE, r, bias & 95% CI are considered to validate the proposed method. To explore the relevance of proposed physiological features with the blood pressure, genetic algorithm(GA) with the random forest model is employed.
Results: Significant features like alpha, QRS complex, QT interval, SDI, heart rate are acquired. The best optimal feature set from GA reduced the MAE from 13.20 to 9.54 mmHg, 9.91 to 5.48 mmHg, 7.71 to 3.37 mmHg for SBP, DBP and MBP respectively.
Conclusion: Model build with ECG and PPG time-domain features outperform the model trained with PPG features alone. Results obtained from GA validates the significance of ECG features correlation with BP.
Significance: Identifying the associations of ECG features with BP helps in selecting relevant features which minimize the computational cost as well as errors in the assessment of BP.

1. Introduction

Blood pressure (BP) is one of the vital signs to be monitored to diagnose the subject's health conditions. Raised blood pressure, known as hypertension (HTN) is one of the cardinal risk factors associated with the cerebrovascular accident (CVA), cardiovascular diseases, and renal impairment which is estimated to affect 1.5 billion people worldwide [1]. Treating the complications of HTN at an early stage entails the nation's economic gains and prolonged life expectancy. Continuous and accurate blood pressure measurement is fundamental to the management of HTN. Mercury Sphygmomanometer, a long-established, non-invasive, golden standard of BP measurement, uses the inflatable cuff. While the cuff is deflated, the kortokoff sound is monitored using a stethoscope. In the invasive method, intra-arterial BP is considered a significant technique where the catheter is inserted into the aorta. However, as it is prone to infections, this method limits its clinical use. The oscillometry method is also a well-established method to estimate BP using a maximum amplitude algorithm. In this technique, the small oscillations are extracted, and its envelopes are computed which give the estimation of systolic blood pressure (SBP) and diastolic blood pressure (DBP) [2]. However, both the techniques provide the intermittent BP, constrict the blood flow and require trained technicians. In addition, the volume clamping method and the tonometric method uses the finger cuff to reconstruct the blood pressure values. However, the placement of the sensor on the exact location of the artery is challenging in tonometry [3].

The techniques mentioned above have their drawbacks, which result in the emerging principle called pulse wave velocity (PWV) based BP measurement. For instance, the cuff-based measurement

* Corresponding author.
E-mail address: guma@nitt.edu (U. Gandhi).

https://doi.org/10.1016/j.bspc.2020.101942
1746-8094/

of blood pressure causes discomfort in the case of ambulatory monitoring, inappropriate cuff sizing and provides an intermittent measurement. Hence, cuffless BP assessment based on Pulse transit time (PTT) is evolved to overcome the demerits associated with the cuff based measurement. The three most cited algorithms based on PTT paved the way for continuous and cuffless blood pressure measurement. Chen et al. estimated the SBP by obtaining change in pulse transit time along with intermittent calibration values. However, he observed a reduction in accuracy when the calibration interval is longer [4]. Poon et al. replaced the elastic modulus with Hughes equation and calculated SBP and DBP [5]. Although the above two algorithms estimated blood pressure, the diameter is set aside as a constant parameter. In 2015, Ding et al. proposed the new indicator, photoplethysmogram intensity ratio (PIR) which reflects the vasomotor tone, change in arterial diameter as well as it could track both high and low frequency variations in BP [6]. In physiological terms, blood pressure is regulated by cardiac output and total peripheral resistance, which include vessel diameter, blood viscosity, and vessel length and blood volume. Therefore, a novel BP algorithm based on Morgan and Kiley expression as a principal equation was modelled which relates pulse wave velocity with the elastic modulus, arterial wall properties, and α parameter that reflects the fluid flow with respect to viscous effects. After examination of the same, accuracy was improved in BP estimation for both healthy and diseased subjects [7].

Regardless of the pioneering work in the area, all of these approaches require subject-based calibration and are inferior in accuracy in long term BP tracking. In this context, machine learning is considered more efficacious to assess the blood pressure using physiological signals like ECG and PPG and is becoming widespread, as it does not require frequent calibration. Since vessel elasticity, peripheral resistance, blood volume and cardiac output influence blood pressure, one of the new-fangled ways in machine learning research is the inception of features [8,9] which reflect the various physiological phenomena mentioned above. It is observed that blood pressure monitoring becomes more effective when these features, which are extracted from ECG and PPG, are used as an input for the regression technique.

In this study, we propose a novel feature, the Womersley number that reflects the flow properties of the blood. Also, features like systolic diastolic interval interaction (SDI), amplitude and time-domain features are extracted from the ECG, and morphological features from the pulse signals are used to build various machine learning models and its results are compared with the conventional methods of cuffless blood pressure monitoring. However, the extracted feature set needs to be leveraged to improve the accuracy of the blood pressure estimation using ML models. Hence, genetic algorithm along with Random Forest (RF) is employed to acquire the optimal feature subset. On the whole, the attempt is to uncover the potential associations between these features and blood pressure using an optimization technique combined with an RF model for the accurate estimation of BP.

2. Background

Machine learning (ML), an application of artificial intelligence (AI) brings a paradigm shift in medicine attribute to the enhancement in pathologic diagnosis, patient monitoring, assisting in surgery, complex interpretation and decision-making act in the required domains [10]. Numerous previous studies reported the link between PTT, PIR, HR and BP using ML models. Fung et al. developed a model, which addresses the tracking of BP during the administration of drugs and surgical simulation [11]. It relates the BP to the inverse square of PTT, and it is given by,

$$BP = \frac{1}{PTT^2} + B \tag{1}$$

Subsequently, in PTT and BP relation trends, not only PTT but HR also contributes to the estimation of BP and found improvement in performance. Authors also propose the adaptive calibration, which tunes the model parameters once it exceeds the calibration interval tolerance time [12]. The requirement of individual calibration at different physiological states to obtain a calibration curve is one of the tailbacks though PTT is a good surrogate for BP estimation. Yan and Zhang improve this by proposing the novel calibration method based on the effect on arteries by the applied external pressure and found the good repeatability till two months [13]. Wong et al. in their research investigated the relationship between the pulse transit time and BP on 14 subjects and a half year later, the repeatability test was conducted using the same coefficients to analyze how good the prediction is compared to the first test. It is understood that coefficients obtained half a year ago could not obtain the BP well [14]. Kachuee et al. [15] proposed the PPG based whole parameters and physiological based features which are extracted from ECG and PPG to improve BP estimate using ML models. The authors also presented the scheme to eliminate the subject-based calibration. Xing and Sun et al. [16] in their work that investigated the intrinsic connection between PPG and BP and proposed a mathematical equation to describe their relation, efface the influence of subject-specific contribution based on proper normalization.

Bing Zhang et al. proposed the effective method for continuous BP measurement using support vector regression and evaluated the model using six evaluated indices by comparing with classic ML algorithms Linear R and back propagation neural network (BPN). The feature selection and analysis are done using Spearman's correlation coefficient and the Mutual Information coefficient. Thus, the close association between PTT, HR & PPG features and BP is found [17]. Fen Miao et al. projected the relation between morphological features extracted from ECG and PPG with BP using MLR and SVR models. The best feature set is selected based on the filter and wrapper methods. The model is validated on the static, dynamic and follow-up on the experiment after 6 months [18]. Ahmadreza et al. [19] assessed BP successively using wrist and fingertip photoplethysmogram based on ANN. The optimal feature set obtained by the genetic algorithm to investigate the most important features that influence the BP also estimated separate feature sets for SBP and DBP. The feature set also includes the other demographical data like age, gender, height, and weight. In due progression, the blood pressure estimation using PPG alone started flourishing as it doesn't require the involvement of ECG signal. Kruylyak et al. [20] extracted the 21 PPG features, which reflect the physiological indices, and ANN model was used which demonstrated the improvement in accuracy with PPG features.

All of the above-mentioned approaches explored PPG features along with PTT and demographic information of the subject and complexity features [21] as well for estimation of BP. Few previous studies made an effort to explore the relationship between ECG signals and BP [22–25]. Many authors have reported the incidences of left ventricular hypertrophy, which require the prompt intervention with hypertension to prevent further cardiovascular complications [26,27]. On that account, this study, to our knowledge, is a first attempt to use ECG time-domain features and Womersley number along with PPG features to estimate BP.

3. Methods

Fig. 1 shows the block diagram of the entire approach to obtain the estimation of cuffless BP. The following steps are done to estimate BP. (1) ECG and PPG signals are obtained from the public dataset. (2) Pre-processing of the signal is performed to eliminate

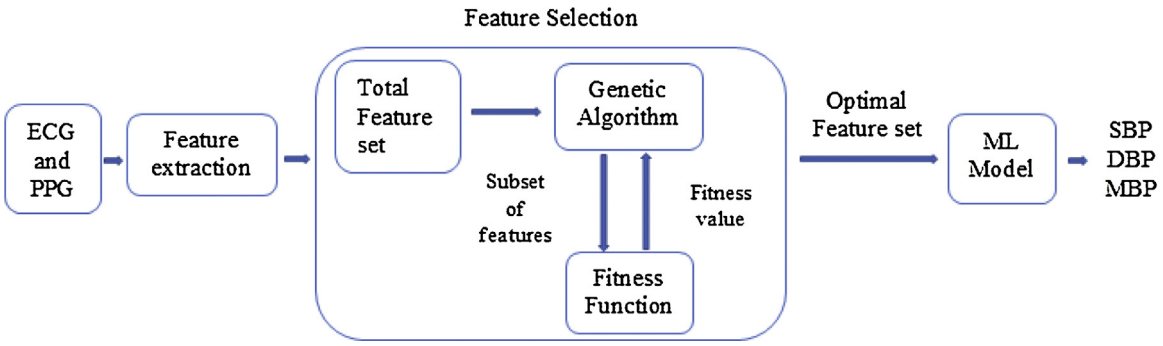

Fig. 1. Block diagram of a proposed cuff less BP measurement system.

the noise. (3) Features are extracted from ECG and PPG. (4) Feature derived is aided as an input to various regression models. (5) Genetic algorithm is used to acquire optimal feature sets for better accuracy. The above process is elaborated in the following sections.

3.1. Online database

The database from UCI machine learning repository, center for machine learning and intelligent systems is considered to design the model for cuffless blood pressure estimation. This dataset is actually a processed version of the Multi-parameter Intelligent Monitoring in Intensive Care (MIMIC) II online waveform database [28] provided by PhysioNet organization. The processing that is followed to derive the UCI dataset from the MIMIC II dataset has been explained in [29]. The database consists of ECG acquired from bipolar limb lead configuration II channel, PPG using finger plethysmogram and IABP (Intra Arterial Blood Pressure) signals from 12,000 instances sampled at 125 Hz. The ABP signals are considered as the ground truth from which SBP and DBP are calculated. In total, there are 12,000 data of which after removing certain subjects' data whose records with very high BP or very low BP was removed (SBP>=180, DBP>=130, SBP<=80, DBP<=60) and filtering process, we end up in 3801 data signals each of them is attributed to unique ID. The limit is chosen to compare our work with [29] conventional literature. The database is in the format of MAT files consisting of cell of array matrices where each cell represents the single individual record. Since each record has a varying record duration, careful visualization of first 1000 samples are considered as some of the records in the database possess a maximum of 1000 samples and also most of the signals are distorted towards the end. Each instance is also given a unique ID to prevent overlapping of the data in the dataset. The dataset is then split into 80% for training and 20% testing. Thereafter, the signals are pre-processed before it is used to build a machine-learning model. The 3rd order Butterworth bandpass FIR filter is used to eliminate the artifact in the signals. The signal is also corrected for the 50 Hz noise. Fig. 2 shows the distribution of the target values in the final dataset.

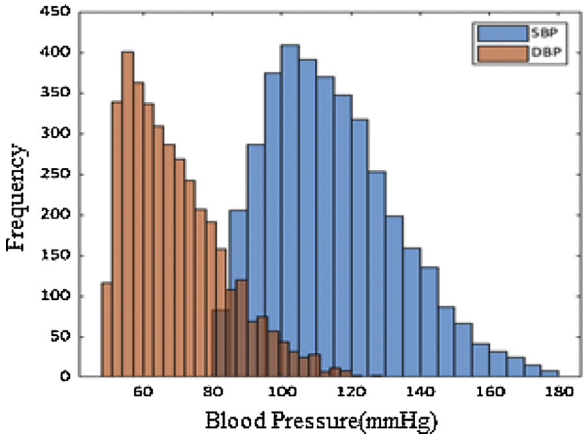

Fig. 2. Distribution of BP values.

3.2. Feature extraction

Based on the previous study reports and features introduced in this study, total of 43 features were extracted from the pulse, ECG, and combination of ECG and pulse signal using Matlab R2019a, and it is tabulated in Table 1. The following sub section explains the feature extraction from the signals in detail.

3.2.1. Pulse arrival time and PIR

Pulse Arrival Time (PAT) is considered as the critical marker of arterial blood pressure. The pulse arrival time (PAT) which is defined as the time taken for the blood to reach the periphery from the aorta is acquired using cross-correlation between ECG and sparsified PPG signals. Sparsification of PPG signal is done by moving window maximum of the PPG signal and only the maxima are retained which results in the sparse signal. Now, the PAT can be extracted by considering three points in the pulse signal and the R wave of ECG [15]. PIR represents the arterial diameter change [6] which is derived from the signal. It is defined as the ratio of the maximum to minimum intensity of the pulse signal.

3.2.2. Womersley number (alpha)

The Womersley parameter is the ratio of inertial force (pulsatile frequency) to viscous effects. When α is low, the viscous force tends to dominate and in turn, affects the blood pressure in case of pathological conditions even in larger arteries. Therefore, the number, which gives information about the viscous flow, can be acquired from the signal in two ways:

a. Extraction of Womersley parameter, $\alpha = R\sqrt{\frac{\rho\omega}{\mu}}$, R is taken as the diameter of the vessel during systole, where ρ is density of blood-1060 kg/m^3 kept constant, ω is frequency of a heart rate (HR) and μ is viscosity of blood from the pulse signal are as follows:

PIR, a recently proposed novel indicator [30] reflects the arterial diameter change which is one of the important sources of systemic vascular resistance. It is a ratio of PPG peak to valley intensity. During systole, the arterial diameter (D_s) increases so the incident light intensity will be absorbed by the blood in the vessels, hence transmitted light intensity will decrease to a minimum value (I_L). During diastole, the arterial diameter (D_s) decreases so the incident light intensity will be absorbed by the minimum blood in the vessels, hence transmitted light intensity will increase to a maximum value (I_H). Therefore, to calculate Womersley number, R is considered to

Table 1
Feature name and its definition.

Feature Name	Definition
PIR	Photoplethysmogram intensity ratio, ratio of maximum and minimum amplitude of the pulse signal
Ih	maximum amplitude of the pulse signal
Il	minimum amplitude of the pulse signal
Meu_o	Viscosity of the blood, calculated as AC amplitude of the pulse signal.
Sw10	Systolic width @ 10% of the pulse amplitude
St10+Dt10	Addition of Systolic time and diastolic time @ 10% of the pulse amplitude
Dt10/St10	Division of Diastolic time and systolic time @ 10% of the pulse amplitude.
St25+Dt25	Addition of Systolic time and diastolic time @ 25% of the pulse amplitude
Dt25/St25	Division of Diastolic time and systolic time @ 25% of the pulse amplitude.
St33+Dt33	Addition of Systolic time and diastolic time @ 33% of the pulse amplitude
Dt33/St33	Division of Diastolic time and systolic time @ 33% of the pulse amplitude.
Dt50/St50	Division of Diastolic time and systolic time @ 50% of the pulse amplitude.
St	Systolic time
Dt	Diastolic time
AI	Augmentation Index
LASI	Large artery stiffness ratio
S1,S2, S3, S4	Inflection point area ratio
PAT_d, PAT_f, PAT_p	Pulse arrival time
Meu_n	Viscosity of the blood calculated based on pulse pressure wave propagation
Omega (frequency of HR)	The frequency of heart rate
$Alpha_o$	Womersley number
$Alpha_n$	Womersley number(2^{nd} method)
SDI	Systolic Diastolic time interval
SDI_n	New systolic diastolic interval
QT_c	The time interval between Q and T of ECG corrected for heart rate.
RR	The time interval between two successive R wave of ECG
QT	The time interval between Q and T of ECG
TQ	The time interval between T and Q of successive ECG
PR	From the start of the P wave to the start of the QRS complex
QR	From the start of the Q wave to the start of the QRS complex
QRS	From the start to the end of the QRS complex
P	Amplitude of P wave and it represents the atrial depolarization
Q	Amplitude of Q wave, negative deflection of QRS complex
R	Amplitude of R wave and it represents the ventricular depolarization
S	Amplitude of S wave
T	Amplitude of T wave and it represents the atrial repolarization
SDI_c	Systolic diastolic interval corrected for RR interval
HR	Heart rate

be I_L (valley intensity) of the PPG signal, as it implies the maximum extent the artery can dilate to hold the blood during systole.

There are few literatures which analyse the PPG in relation to hemorheological properties and found that some features in the PPG pulse signal helps us in estimating the systemic vascular resistance. Njoum et al. in their work [31] investigated the effect of fluid viscosity on AC and DC component of PPG signals using pulsatile pump. It is seen from the results that fluid 1 shows enhanced AC amplitude than fluid 2 which is more viscous than fluid 1 and it is concluded that AC amplitudes are sensitive to the changes in fluid viscosity. They also found the strong correlation of 0.97 between PPG_{AC} components and fluid viscosity. Hence, in this work, the peak amplitude of PPG's AC signal is considered as a substitute for viscosity.

b. Inspired from Wei's work [32], where spring constant that was ascribed to the arterial stiffness is derived non-invasively to notice the peripheral arterial elasticity based on the arterial pressure wave equation given as,

$$\frac{d^2P(z,t)}{dt^2} + b\,\frac{dP(z,t)}{dt} + K\,P(z,t) = -V_\infty^2\,\frac{d^2P(z,t)}{dz^2} \tag{2}$$

Where P(z,t) is the pressure term and it is defined as the difference between the internal fluid pressure and fluid pressure in the static condition. b – damping coefficient which is related to the viscosity of the fluid and artery wall as well as size of the artery wall, k – spring constant. V^2 – external force due to the windkessel effect. Wei, in his work used strain gauge pressure sensor on radial artery to detect the pulse waveform under optimum contact pressure. From the above equation, the following spring constant is derived as,

$$K = -\frac{\frac{d^2x(t_{peak})}{dt^2}}{x\left(t_{peak}\right)} = -\frac{EF}{BD} \tag{3}$$

Where K – spring constant, EF denotes the magnitude of the second derivative of pulse signal at point C and BD represents the displacement between corresponding point B and C. $x\left(t_{peak}\right)$ is a peak of an arterial pulse, $\frac{d^2x(t_{peak})}{dt^2}$ is a peak of the second order derivative of arterial pulse waveform.

However, in this study we used finger photoplethysmograph to find out the spring constant k as suggested in [32] and friction coefficient, b from Eq. (2). Since, p is a slowly varying function of z, the term can be neglected based on first order approximation and add the unit impulse term [33] to find the value of b. Therefore, Eq. (2) can be transformed as the following [32]

$$\frac{d^2x(t)}{dt^2} + b\,\frac{dx(t)}{dt} + K\,x(t) = 1 \tag{4}$$

Where $x(t)$ is the displacement of the arterial wall. Since the damping force is high at point B of the pulse signal, with the impulse response the value of b is found by substituting Eqs. (3) in (4) which gives,

$$b = \frac{1 - Kx(t_{peak}) - \frac{d^2x(t_{peak})}{dt^2}}{\frac{dx(t_{peak})}{dt}} = \frac{1 - (K * BD) - EF}{GH} \tag{5}$$

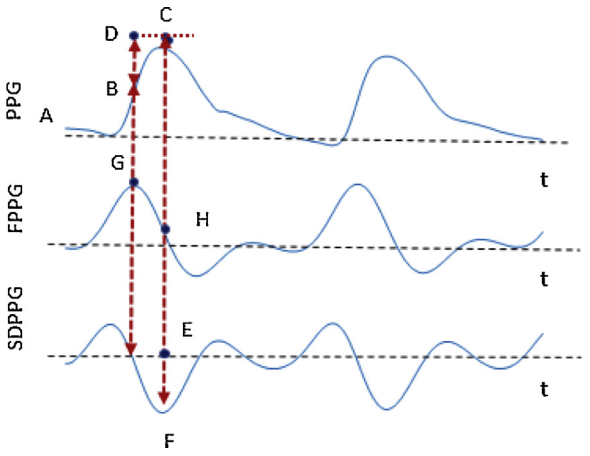

Fig. 3. Representation of arterial pulse separated by points along with its first (FPPG) and second derivative (SDPPG). A is the valley of the arterial pulse, B is the maximum slope of the pulse and C is the peak of the pulse. D is the equivalent point of C, *EF* denotes the magnitude of the second derivative of pulse signal at point C, *GH* denotes the magnitude of the first derivative of pulse signal at point C.

Where GH denotes the magnitude of the first derivative of pulse signal at point C and $\frac{dx(t_{peak})}{dt}$ represents the first order derivative of pulse waveform. The term K*BD and EF cancels out each other and damping coefficient b, is estimated as an inverse of the first derivative of the pulse signal. The Fig. 3 shows the extraction of damping coefficient from the arterial pulse and derivative.

In the present study, damping coefficient b is used to obtain the viscosity of blood (μ) by assuming that the viscosity of the artery walls and the size effect of the artery walls do not affect b. Therefore, the friction, given by the damping coefficient is assumed to be directly proportional to the viscosity of the fluid. Hence it may be written as

$$b \propto \mu \quad \text{or} \quad b = k\mu\,. \tag{6}$$

This assumption is based on the study of liquid flow in tubes from classical hydrodynamics where the friction coefficient is found to be directly proportional to the viscosity of the fluid [34]. In general, the friction coefficient in a fully developed pipe flow is given by Fanning friction factor formula [35], which may be written as

$$f = \frac{\Delta P\, D}{LV^2\, \rho} \tag{7}$$

Where ΔP is pressure difference which is given by $\Delta P = \frac{32\mu VL}{D^2}$, D is Diameter of the vessel, L is the length of the tube, V is Velocity of the fluid, ρ- density of the fluid and μ is the viscosity of the fluid. Substituting ΔP in Eq. (6), it is implicit that the friction coefficient is a function of viscosity. It can be written as,

$$f \propto \mu \quad \text{or} \quad f = k\mu \tag{8}$$

By comparing Eqs. (6) and (8), it is clearly seen that within the framework of the present assumption, $b = f$. Therefore, the constant k can be calculated as $= \frac{32}{V\rho D}$. Substituting $\frac{b}{k} = \mu$, in womersley number, the equation becomes,

$$\alpha = \sqrt{k}\, R\sqrt{\frac{\omega\rho}{b}}$$

The order of magnitude of Womersley number depends on the order of magnitude of k. To find the magnitude order of k, it is calculated for a general case where the average density of the blood is chosen as 1060 kg/m^3, the range of diameter of the aorta artery is taken as 0.020–0.035 m [36] and peak velocity of blood in aorta is taken to be 1.50–1.75 m/s [37]. Based on these values, the magnitude of k is obtained to be approximately 1 Ns/m^2 [Range being 0.5–1 N s/m^2]. Since the range of k is close to 1 Ns/m^2, its square root will be much closer to 1. Therefore, the magnitude of k as well as its square root is of order 1. With this it can be concluded that $\sqrt{k}$ may be dropped in the subsequent analysis to estimate the womersley number without significant change in its order of magnitude. Therefore, the equation for α is written as,

$$\alpha = R\sqrt{\frac{\omega\rho}{b}} \tag{9}$$

After the extraction of b from pulse signal, R was extracted as valley amplitude of the pulse signal to acquire α.

3.2.3. ECG based features

The ECG features extracted from the signal are represented in the Fig. 4a). The time-domain features like QRS complex, PR interval, amplitude of P, Q, R, S, T, heart rate, RR interval, QR interval, QT interval, QT interval corrected for heart rate, TQ interval, Systolic diastolic interval (SDI), SDI corrected for heart rate are extracted from the ECG signal. Some of the features, which are not embodied in the Fig. 4a) is elaborated as follows:

3.2.3.1. QTc interval. Since QTc interval is associated with mean blood pressure [38], Bazzet's formula is used to correct the QT interval for heart rate and it is given as,

$$QT_c = \frac{QT}{\sqrt{RR\ interval}} \tag{10}$$

3.2.3.2. Systolic and diastolic interval interaction (SDI). SDI is extracted based on two methods proposed in the literature [39,40]. Fossa et al. define SDI as a ratio of QT and TQ interval within each cardiac cycle. Concurrently, Imam et al. defines the ratio of QT and RR interval, named as SDIn in this work. In addition, SDIc, defined as the corrected SDI for heart rate.

3.2.4. PPG based features

The 20 features of PPG signal are obtained based on [20] such as systolic upstroke time (SUT) and diastolic upstroke time (DUT), and the ratio of SUT and DUT. However, only 10 features are finalized since rest of the features which are closer to zero were neglected. The physiological features obtained from pulse signal are shown in the Fig. 4b). The features extracted are based on [15].

3.3. Regression methods

Once the features are extracted, the following are the various machine learning models considered to find the possible association between input features and the blood pressure. The feature vectors are trained using all the models and compared with each other. Also, separate models are trained for estimating the targets such as SBP, DBP and MBP.

3.3.1. Linear regression

Linear Regression is a simple regression used for predictive modelling and easy to implement as well. It gives an equation with slope and intercept that predicts the target values. The relation between BP, denoted as Y and input features as $x_1, x_2, \ldots x_n$ are expressed in the equation

$$Y = \alpha_o + \alpha_1 x_1 + \alpha_2 x_2 + \ldots\ldots \alpha_n x_n \tag{11}$$

where $\alpha_1, \alpha_2, \ldots \alpha_n$ are coefficients obtained from the model.

3.3.2. Ridge regression

It is also called regularization technique. Here, the Ordinary Least square (OLS) loss function is augmented in such a way that we

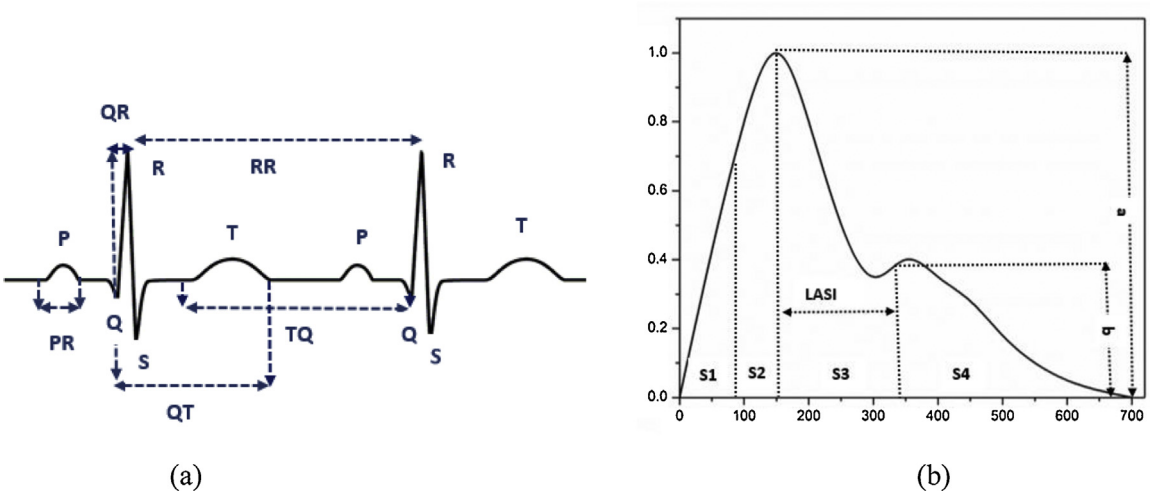

Fig. 4. Representaiton of a) ECG and its features b) Physiological based features.

not only minimize the sum of squared residuals but also penalize the size of parameter estimates, in order to shrink them towards zero. As model complexity increases, parameter estimates increase exponentially. Hence, constraint on model coefficients will reduce the model complexity.

3.3.3. Support Vector regression

Unlike simple linear regression, this helps to minimize the errors within the boundary line by separating the dataset using the hyperplane. The kernel function is used to transform the data into higher dimension to perform the linear separation. Support vector regression uses support vector machine, which constructs the hyperplane between the data points which is the best fit line that has maximum number of points [41]. Radial basis function is used as a kernel and Sci-kit library is used to train the regression model.

3.3.4. Adaboost regression

It is the boosting algorithm, i.e., it can be combined with any other machine learning algorithms to improve the performance. It combines all the weak learners to predict the target value. Predictions are made by calculating the weighted average of the weak classifiers. Here, 1000 number of decision trees are used to train a model. It is also less susceptible to the overfitting problems.

3.3.5. Random forest regression

Random forest Regression is one of the most effective models of machine learning for predictive analysis. It is good at estimating the output even when the features are in non-linear relation with targets. RF also reduces the overfitting, i.e., it reduces the variance-bias trade off by combining the predictions of every decision tree. Diversity in every tree results in the robustness of the model. Sci-kit library is used to train the regression model.

3.4. Feature selection

Among various machine learning algorithms, the best model that provides least error is considered to combine with genetic algorithm (GA) to obtain the optimal feature set separately for SBP, DBP and MBP. In the present study, the feature analysis using Binary GA is implemented to find the possible best combination of features by discarding irrelevant features and construct a model effectively to improve the accuracy in estimation of SBP, DBP and MBP. The initial population was generated randomly and updated at every iteration. The chromosome length is 43, which consists of 0's and 1's indicates its absence and presence of features respectively. The inverse of mean absolute error from the ML model is considered as the fitness function.

4. Results

The time-domain features are extracted from the ECG and PPG signals for the continuous cuffless blood pressure estimation. The feature set consists of novel features like Womersley number, SDI, QRS and QT_c interval are employed for the purpose of minimizing the error in BP estimation as well as to explore its associations with the BP. The 43 features are fed into various machine learning models like linear regression, ridge regression, support vector regression, adaboost regression, random forest regression and evaluation metrics such as Root mean squared error (RMSE), Mean absolute error (MAE), Mean Squared error (MSE), Bias and its 95% Confidence Interval (CI), Intraclass correlation coefficient (ICC), Correlation Coefficient (r) are calculated.

The following Table 2 shows the comparison of MAE and RMSE on various ML algorithms. Different combinations of features are investigated to demonstrate the improvement in performance due to the proposed features on various ML algorithms. It is comprehended that MAE and RMSE of Random forest model is comparatively better for different feature combinations. It is also apparent that ECG features along with PTT provide least MAE and RMSE for RF model compared to other combinations, which accounts for better BP assessment.

Table 3 shows the RF model performance with and without ECG features and alpha. It is also implied that the evaluation metrics are augmented when the feature set comprised of ECG features indices. Smaller MAE, bias and better correlation coefficient are observed for the feature set that contains ECG features. The 95% CI of bias shows the wider interval range for feature set without ECG compared with the feature set encompasses ECG indicates its significance in BP estimation.

The data was checked for the assumption of normality using Shapiro Wilko test and found statistically significant. The statistical significance test was estimated using Student's lower tailed paired *t*-test and $P < 0.05$ is regarded as statistically significant. The significance test was performed between MAE of ground truth control (IABP), all features and MAE of ground truth, feature set without considering the features of ECG and womersley number for SBP (t value: −4.335 and p value: 0.00001), DBP (t value: −5.413 and p value: 0.00000) and MBP (t value: −3.673 and p value: 0.00013). Intra class correlation coefficient (ICC) was calculated using SPSS software for assessing the agreement between two clini-

Table 2
Comparison of performance of various ML methods using different feature set.

BP	Feature set	Machine Learning Techniques									
		Linear Regression		Ridge Regression		Support Vector Regression		Adaboost Regression		Random Forest Regression	
		MAE	RMSE	MAE	RMSE	MAE	RMSE	MAE	RMSE	MAE	RMSE
SBP	ALL	14.05	17.78	14.23	18.04	14.85	18.92	14.20	17.17	10.83	14.96
	PTT + PPG features	15.27	18.90	15.19	18.94	15.14	19.30	15.63	19.17	14.14	18.18
	Physiological features	15.13	18.84	15.10	18.90	14.70	19.04	16.90	20.07	11.89	15.88
	PTT + ECG features + alpha	15.06	18.91	15.08	18.81	14.94	19.07	16.18	19.44	11.16	15.00
DBP	ALL	10.76	13.92	10.94	13.92	10.98	14.41	11.99	14.32	8.43	11.62
	PTT + PPG features	11.37	14.38	11.41	14.31	11.17	14.61	12.52	14.98	10.58	13.73
	Physiological features	11.06	14.05	11.40	14.30	11.08	14.51	11.81	14.36	9.38	12.54
	PTT + ECG features + alpha	11.35	14.33	11.21	14.12	11.05	14.47	12.11	14.45	8.55	11.84
MBP	ALL	10.44	13.28	10.59	13.30	10.70	13.76	10.95	13.07	8.35	11.05
	PTT + PPG features	11.19	13.86	11.14	13.77	10.95	14.01	12.06	14.36	10.22	13.12
	Physiological features	10.86	13.58	11.09	13.76	10.77	13.95	11.27	13.55	9.11	11.91
	PTT + ECG features + alpha	11.08	13.79	10.95	13.60	10.75	13.83	11.96	14.10	8.45	11.33

Table 3
Performance comparison of feature set with and without ECG features for RF model.

BP	Feature set	MAE	RMSE	ICC‡	r‡
SBP	All features	10.83	14.58	0.70 (95% CI: 0.64–0.73)	0.64
	All features without ECG features and alpha	11.53	15.32	0.60 (95% CI: 0.55–0.66)	0.54
DBP	All features	8.40	11.01	0.66 (95% CI: 0.60–0.70)	0.61
	All features without ECG features and alpha	9.22	11.92	0.57 (95% CI: 0.50–0.62)	0.51
MBP	All features	8.25	10.77	0.65 (95% CI: 0.60–0.70)	0.61
	All features without ECG features and alpha	8.86	11.32	0.57 (95% CI: 0.53–0.65)	0.56

‡ICC – Intra class correlation coefficient. ICC values less than 0.5 are indicative of poor reliability, values between 0.5 and 0.75 indicate moderate reliability, values between 0.75 and 0.9 indicate good reliability, and values greater than 0.90 indicate excellent reliability.
‡r – Pearson Correlation Coefficient, CI‡ – Confidence Interval.

cal evaluation methods. It is observed that degree of agreement and correlation is slightly less for the feature set without ECG and alpha validates its association with BP.

The Bland Altman (BA) plot was generated signifying the mean difference and average BP to show the agreement between the estimated and reference method. The mean difference and the limits of agreement are seen in the following Fig. 5. The Pearson correlation for SBP, DBP and MBP is 0.64, 0.61, 0.61 respectively and it is exemplified in the following regression plot. From the plot it is obvious that maximum number of observations is within the limits of agreement demonstrates the consensus between estimated and reference method. However the limits of agreement were too wide to consider it as clinically significant when all the features were given to the model.

Therefore, GA was used to discard the unimportant features to minimize the estimation errors. GA with an initial population of 100*43, with a mutation rate of 0.25%, and the single point crossover is implemented. Since fitness function is the inverse of MAE of RF model, it repeatedly calls the algorithm and generates the model every time (number of time it calls is depends on the population rate) which ends up in computational complexity and cost as well. Considering the limitations in practical applications, after many trials with an original dataset, the dataset size is reduced to 100*43 and fed into search technique combined with RF model to obtain the best subset from the feature set, which ends up with many ECG features and alpha. It is also well reflected in the reduction in MAE of SBP, DBP and MBP as compared to the RF model with complete feature set. The results of the GA algorithm further aid us to conclude that some of the ECG features are strongly associated with the BP and it is shown in the following Table 4.

For the dataset of size 100*43, the genetic algorithm is applied, optimized feature subset is obtained, and results are compared. The results for all the 43 features as well as the results of the GA given to RF model are tabulated in the Table 5. It is revealed from the table that subset obtained from GA lessens the MAE twice for DBP and MBP as that of all the features used. The correlation coefficient is also improved upon employing the optimal subset.

It is evident from the Table 5 that feature set before and after GA shows the noticeable variations in metrics like MAE, RMSE and r. It is important that since ICC is also fallible, ICC estimates and 95% CI was estimated to show the degree of agreement and reliability. It is observed that before GA, the ICC shows the moderate reliability whereas after optimal feature set ICC indicates excellent reliability.

The statistical significance test was estimated using Student's upper tailed paired *t*-test between MAE of ground truth, before GA feature set and MAE of ground truth, after GA feature set and found that to be statistically significant ($p < 0.05$) for SBP(t value: 2.954 and p value: 0.00408), DBP(t value: 3.496 and p value: 0.00121) and MBP(t value: 2.836 and p value: 0.00527). It is important that introduced feature set needs to be also clinically significant. Hence, Cohen's d ratio was calculated to know the magnitude of an effect size upon the blood pressure due to the optimal feature set and it is found to be 0.345 for SBP, 0.495 for DBP and 0.597 for MBP which in turn validates its substantial clinical effect size.

5. Discussion

Though numerous previous studies investigate the relation between features and vital signs using various ML algorithms, in this study, novel parameters such as Womersley parameter, QRS complex, QT interval, SDI are proposed and employed for the measurement of blood pressure. Further, an effort to analyse the interrelation between ECG features and BP is also demonstrated. Genetic algorithm is chosen as feature selection technique to obtain the best possible feature subset and feed into RF model, which

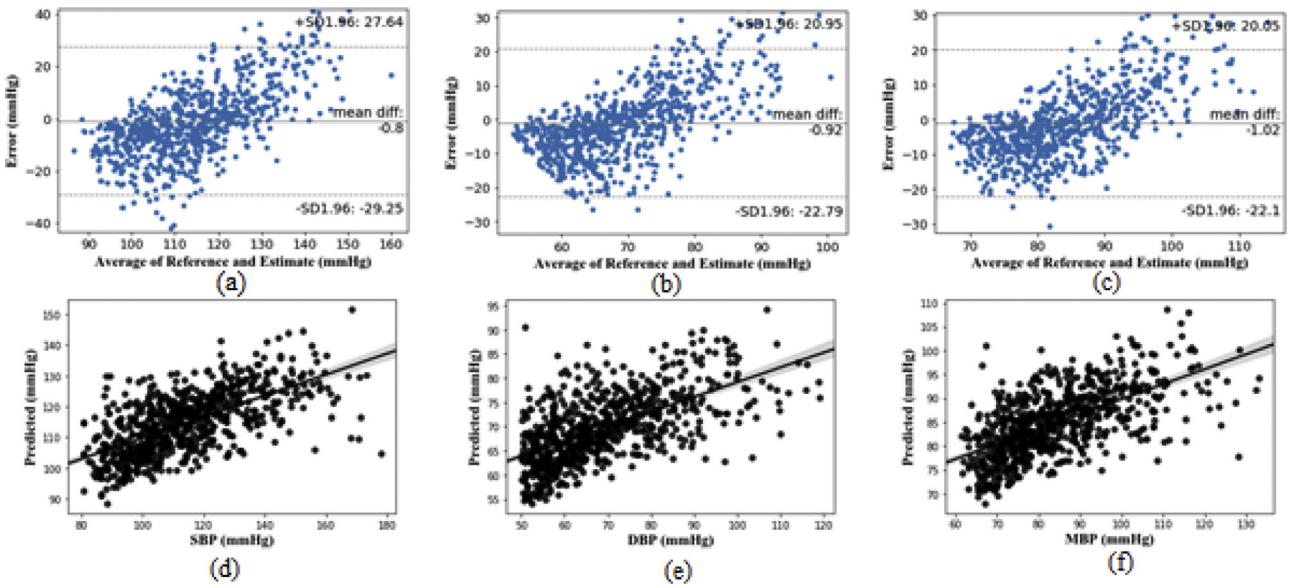

Fig. 5. Bland altman plot showing mean difference and 95% limits of agreement (a) SBP (b) DBP (c) MBP and Regression plot with correlation, r = 0.64, 0.61, 0.61 for d) SBP e) DBP and f) MBP respectively.

Table 4
Optimal feature subset obtained by GA.

SBP	DBP	MBP
PTT,	Ih	PIR
ih,	Il	Ih
systolic width @10%,	systolic width @10%,	Il
@ 10% systolic time + diastolic time,	@ 10% systolic time + diastolic time,	systolic width @10%,
@ 10% diastolic time/systolic time,	@ 10% diastolic time/systolic time,	@ 25% systolic time + diastolic time,
@ 25% systolic time + diastolic time,	@ 25% systolic time + diastolic time,	@25% diastolic time/systolic time
@25% diastolic time/systolic time	@25% diastolic time/systolic time	@33% diastolic time/systolic time
@ 50% Diastolic time/Systolic time,	AI	@ 50% Diastolic time/Systolic time,
AI	Meun	Diastolic time
LASI	Omega	AI
S1	Alphan	S1
S2	SDI	PATd
S4	QTc	PATf
PATf	QRS	PATp
meun	Q	Omega
alphan	R	Alphao
SDIn	T	SDIn
QT		QTc
QRS		QRS
P		P
S		
T		
HR		

Table 5
Results of Random forest model before and after GA.

RF Model	ALL (43 features)				GA's feature subset			
	MAE	RMSE	r	ICC & 95% CI	MAE	RMSE	r	ICC & 95% CI
SBP	13.53	17.65	0.74	0.78 (0.46–0.91)	9.54	13.83	0.85	0.89 (0.72–0.95)
DBP	9.51	11.58	0.60	0.72 (0.30–0.88)	5.48	6.80	0.87	0.90 (0.76–0.96)
MBP	6.70	7.90	0.86	0.91 (0.75–0.96)	3.27	4.03	0.94	0.97 (0.93–0.98)

provided the least MAE for all the selected features. The following discussions are commented in this regard.

Table 6 shows the comparison of the present study with previous relevant works in the literature. Though the method, dataset, algorithm used is not comparable, its feasibility in reliable estimation of BP is demonstrated.

Kachuee et al. in their work [29] estimated BP through feature engineering of the vital physiological signals using SVM model on MIMIC II database. However, authors have used features only from PPG signals unlike the proposed work which used both ECG and PPG features. Also, the result of this study reveals that all the PPG features do not contribute to the accurate estimation of BP. It is also noteworthy that certain ECG features which are found to be important from this study were not considered in the estimation of BP.

Table 6
Performance comparison with conventional works.

Work	Method	SBP				DBP				MBP			
		MAE	RMSE	r	Bias & 95% CI	MAE	RMSE	r	Bias & 95% CI	MAE	RMSE	r	Bias & 95% CI
Kachuee et al. [29]	SVR	12.38	-	-	-	6.34	-	-	-	-	-	-	-
Kachuee et al. [15]	Random Forest	11.17	–	0.59	–	5.35	–	0.48	-	5.92	-	0.59	-
Attarpour et al. [19]	ANN	4.94	5.87	0.94	-	4.03	5.50	0.84	-	-	-	-	-
Proposed work	Random Forest	9.00	13.83	0.85	−1.2 & (9.35,−5.26)	5.48	6.0	0.84	−2.30 & (0.77,−5.37)	3.2	4.0	0.94	−0.11 & (1.83,−2.07)

The present study is compared with the calibration-free technology of Kachuee's work [15] where feature extraction, i.e., the parameter approach and whole based representation of vital signals are fed into RF model to estimate BP. It is also evident from the optimal subset obtained from GA that all the features in the parameter-based approach [15] are not imperative. However, certain important features like AI, PATd, some of inflection point ratio correlates well with SBP and DBP. The proposed work also found to have enhanced MAE and correlation coefficient upon employing the GA's feature subset.

Attarpour et al., in their work used demographic features like weight and height, were added along with first derivative of PPG features might be one of the plausible reason for the least MAE in both SBP and DBP evaluation [19]. Unifying the demographic features which are most significant predictor of BP along with optimal feature set might augment the BP estimation of the proposed work furthermore. However, the correlation r of DBP [19] matches with the proposed work.

From Table 3, it is clear that inclusion of ECG features helps in better estimation of BP. The frequency of heart rate is correlated with DBP and MBP. The womersley number, a new feature introduced in this study, which deals with the flow properties of blood found to be an important feature in the estimation of SBP, DBP and MBP. Meun which represents the viscosity of blood is also found to be a significant feature.

Systolic features which include the S1, S2 and S4, the area under the PPG curve is in proportion to the stroke volume [42] which in turn profoundly impacts the systolic blood pressure [43]. This may be one of the reasons why S1, S2, S4 are present only in the SBP assessment.

Pulse width is a reflection of both pulse wave velocity and reflected wave velocity. Azad et al., in his paper [44] found that pulse width emulates the systemic vascular resistance correlates well with both systolic and diastolic BP rather than pulse amplitude. Hence, the presence of pulse width in SBP, DBP and MBP of GA optimal subset confirms its prominence in estimation.

The prompt cause for the presence of AI on SBP, DBP and MBP is due to the fact that it represents the wave reflection on the arteries. Blood pressure obtained here is based on the non-linear regression model which may not exactly resemble the central aortic pressure, as the wave reflection occurs at the peripheral site. It is remarkable to know that AI affects both peripheral systolic and diastolic BP but not central systolic BP is congruous with the previous findings [45].

It is also important to observe the presence of Ih and Il in the DBP estimation is consistent with the previous study where low frequency components are perceived in DBP and can be evaluated using PIR, a ratio of Ih and Il. Since MBP is the 2/3 of DBP and 1/3 of SBP, PIR is noted in the MBP estimation. It is imperative to note the systolic peak, ih in the estimation of SBP.

As clearly evident from the Table 4, incorporation of ECG features provides better estimation. It also improves the correlation coefficient. Previous studies that attempted to explore the impact between ECG signals and blood pressure concluded that ECG voltage indices like R, S, T accounts for subsequent hypertension [46]. QRS complex is considered as one of the important parameters to identify chronic manifestation of hypertension such as left ventricular hypertrophy. QTc interval, corrected for heart rate is independently correlated to the blood pressure [47]. Prolonged QTc interval is associated with hypertension. In accordance with the above literature, few ECG features like Systolic Diastolic interaction (SDI), QRS complex, QTc, amplitude of P, R, T are intended as important features from GA. This shows the strong and potential correlation between ECG features and blood pressure.

Of the total features, GA selected 22, 17 and 19 features for the estimation of SBP, DBP and MBP respectively. PAT, ih, Alpha, @25% st + dt, AI, @25% dt/st, SDI, QRS, QT are found as the common features in BP estimation. It is also demonstrated that different feature subsets which were selected by the GA for the estimation of BP is congruous with other outcomes in the literature [19]. It also helps to reduce the computational cost by considering only the best feature subset for the target estimation.

Womersley number which mirrors the influence of fluid flow properties on BP provides the better estimation since it is also one of the determinants of total peripheral resistance. The ECG features are also related to the hypertension identification as cardiovascular disorders like ventricular hypertrophy requires prompt intervention with blood pressure. Hence, unification of pulse features with alpha and ECG features could lead to the improved prognosis in hypertension management. However, there are few constraints related to the present study. First, the dataset analysed comprises of the subjects whose BP is in the range of hypertension, normal and prehypertension. Therefore, the optimal set of features selected by GA for subjects who are in the range of normal and hypertension might vary. Second, owing to the practical limitations involved in computational cost, genetic algorithm with the RF model is applied only to a confined dataset. The larger dataset should be used to authenticate the relation of time-domain based ECG indicators with BP. Thirdly, extraction of R and μ from the pulse signals is an indirect estimation which should be explored further and PAT is used as one of the features which has an effect of PEP. BCG/SCG would facilitate the study of the impact of PEP in BP estimation.

6. Conclusion and future works

Calibration free continuous cuffless blood pressure assessment using machine learning algorithm is still considered to be a matter of debate in terms of feature extraction and evaluation, accurate diagnostics and the like. This study evaluates and compares the performance of various ML methods. The Womersley number (α) along with different ECG and pulse features in the time-domain is considered, and its relevance with BP is also studied. The genetic algorithm provided the most significant features that improved the performance of the model in estimating BP in comparison with all the features given to the model. Though the different feature sets are extracted, the complexity and morphological features of the signal are not explored. Demographic information of the subjects could also improve the performance of BP estimation. Further, inclusion of APG features must be employed in the feature set to obtain a better BP evaluation. Nevertheless, this pilot study explores the hemodynamic alteration effect on BP and integrates ECG voltage and time indices along with pulse signal features that improve the robustness of the model and leads to a reliable estimation of BP.

CRediT authorship contribution statement

Geerthy Thambiraj: Conceptualization, Methodology, Software, Validation. **Uma Gandhi:** Writing - review & editing, Supervision. **Umapathy Mangalanathan:** Writing - review & editing, Supervision. **V. Jeya Maria Jose:** Software. **M. Anand:** Data curation.

Acknowledgment

The authors thank the Ministry of Human Resource and Development (MHRD), Govt. of India for its support.

Declaration of Competing Interest

The authors declare that they have no known competing financial interests or personal relationships that could have appeared to influence the work reported in this paper.

Appendix A. Supplementary data

Supplementary material related to this article can be found, in the online version, at https://doi.org/10.1016/j.bspc.2020.101942.

References

[1] Arun Chokalingam, Impact of world hypertension day, Can. J. Cardiol. 23 (7) (2007) 517–519, PMID: 17534457.
[2] E. Chung, G. Chen, B. Alexander, M. Cannesson, Non-invasive continuous blood pressure monitoring: a review of current applications, Front. Med. 7 (1) (2013) 91–101, http://dx.doi.org/10.1007/s11684-013-0239-5.
[3] B.M. McCarthy, B. O'Flynn, A. Mathewson, An investigation of pulse transit time as a non-invasive blood pressure measurement method, J. Phys. Conf. Ser. 307 (1) (2011), http://dx.doi.org/10.1088/1742-6596/307/1/012060.
[4] W. Chen, T. Kobayashi, S. Ichikawa, Y. Takeuchi, T. Togawa, Continuous estimation of systolic blood pressure using pulse arrival time and intermittent calibration, Med. Biol. Eng. Comput. 38 (5) (2000) 569–574, http://dx.doi.org/10.1007/BF02345755.
[5] C.C.Y. Poon, Y.T. Zhang, Cuffless and Non-invasive measurements of arterial blood pressure by pulse transit time, in: Proc IEEE 27th Annu. Int. Conf. Eng. Med. Biol. Soc., Shanghai, China, 2006, pp. 5877–5880, http://dx.doi.org/10.1109/IEMBS.2005.1615827.
[6] X.R. Ding, Y.T. Zhang, J. Liu, W.X. Dai, H.K. Tsang, Continuous cuffless blood pressure estimation using pulse transit time and photoplethysmogram intensity ratio, IEEE Trans. Biomed. Eng. 63 (5) (2016) 964–972, http://dx.doi.org/10.1109/TBME.2015.2480679.
[7] Geerthy Thambiraj, Uma Gandhi, Viji Devanand, Umapathy Mangalanathan, Non-invasive cuffless blood pressure estimation using pulse transit time, womersley number, and photoplethysmogram intensity ratio, Physiol. Meas. 40 (7) (2019), http://dx.doi.org/10.1088/1361-6579/ab1f17.
[8] X.R. Ding, Y.T. Zhang, Photoplethysmogram intensity ratio: a potential indicator for improving the accuracy of PTT based cuffless blood pressure estimation, IEEE 37th Annu Int Conf Eng Med Biol Soc Milan Italy (2015), http://dx.doi.org/10.1109/EMBC.2015.7318383.
[9] Mengyang Liu, Lai-Man Po, Hong, Cuffless Blood Pressure Estimation Based on Photoplethysmography Signal and Its Second Derivative, 2017, http://dx.doi.org/10.7763/IJCTE.2017.V9.1138.
[10] Kun-Hsing Yu, Andrew L. Beam, Isaac S. Kohane, Artificial intelligence in healthcare, Nat. Biomed. Eng. 2 (2018) 719–731, 10.1038_s41551-018-0305-z.
[11] P. Fung, G. Dumont, C. Ries, C. Mott, M. Ansermino, Continuous Non-invasive blood pressure measurement by pulse transit time, Proceedings of the 26th Annual International Conference of the IEEE EMBS (2004) 738–741, http://dx.doi.org/10.1109/IEMBS.2004.1403264.
[12] Federico S. Catavelli, Harinath Garudadri, Non-invasive cuffless estimation of blood pressure from pulse arrival time and heart rate with adaptive calibration, Sixth International Workshop on Wearable and Implantable Body Sensor Networks (2009), http://dx.doi.org/10.1109/BSN.2009.35.
[13] Y.S. Yan, Y.T. Zhang, A novel calibration method for Non-invasive blood pressure measurement suing pulse transit time proceedings of 4th IEEE EMBS, Internaitonal Summer School Symposium on Medical Devices and Biosensors (2007) 4318–4322, http://dx.doi.org/10.1109/EMBC.2018.8513364.
[14] M.Y. Wong, C.C.Y. Poon, Y.T. Zhang, An evaluation of the cuffless blood pressure estimation based on Pulse transit time technique: a Half year study, Cardiovasc. Eng. 9 (1) (2009) 32–38, http://dx.doi.org/10.1007/s10558-009-9070-7.
[15] M. Kachuee, M.M. Kiani, H. Mohammadzade, M. Shabany, Cuffless blood pressure estimation algorithms for continuous health-care monitoring, IEEE BioMed. Eng. 64 (4) (2017) 859–869, http://dx.doi.org/10.1109/TBME.2016.2580904.
[16] X. Xing, M. Sun, Optical blood pressure estimation with photoplethysmography and fft-based neural networks, Biomed. Opt. Express 7 (8) (2016) 3007–3020, http://dx.doi.org/10.1364/BOE.7.003007.
[17] B. Zhang, Z. Wei, J. Ren, Y. Cheng, Z. Zheng, in: An Empirical Study on Predicting Blood Pressure Using Classification and Regression Trees IEEE Access Special Section on Human-Centered Smart Systems and Technologies, 2018, pp. 21758–21768, http://dx.doi.org/10.1109/ACCESS.2017.2787980, 6.
[18] F. Miao, Nan Fu, Y.T. Zhang, X.R. Ding, X. Hong, Q. He, Y. Li, A novel continuous blood pressure estimation approach based on data mining techniques, IEEE J. Biomed. Health Inform. 21 (6) (2017) 1730–1740, http://dx.doi.org/10.1109/JBHI.2017.2691715.
[19] A. Attarpour, Amin Mahnam, Amir Aminitabar, Hossein Samani, Cuff-less continuous measurement of blood pressure using wrist and fingertip photo-plethysmograms: evaluation and feature analysis, Biomed. Signal Process. Control 49 (2019) 212–220, http://dx.doi.org/10.1016/j.bspc.2018.12.006.
[20] Y. Kurylyak, F. Lamonaca, D. Grimaldi, A neural network based method for continuous blood pressure estimation from a PPG signal, IEEE International Instrumentation Measurement and Technology Conference (2013), http://dx.doi.org/10.1109/I2MTC.2013.6555424.
[21] M. Simjanoska, M. Gjoreski, A.M. Bogdanova, B. Koteska, M. Gams, J. Tasic, ECG-derived blood pressure classification using complexity analysis-based machine learning, Proceedings of the 11th International Joint Conference on Biomedical Engineering Systems and Technologies (BIOSTEC) 5 (2018) 282–292, http://dx.doi.org/10.5220/0006538202820292, HEALTHINF.
[22] I. Mozos, C. Serban, in: The Relation between QT Interval and T-Wave Variables in Hypertensive Patients Symposium-IOMC, 2011, pp. 339–344, 3(3).
[23] Raffaele Marfella, Pasquale Gualdiero, Mario Siniscalchi, Caterina Carusone, Mario Verza, Salvatore Marzano, Katherine Esposito, Dario Giugliano, Morning blood pressure peak, QT intervals, and sympathetic activity in hypertensive patients, Hypertension 41 (2) (2003) 237–243.
[24] J. Klimas, P. Kruzliak, S.W. Rabkin, Modulation of the QT interval duration in hypertension with antihypertensive treatment, Hypertens. Res. 38 (7) (2015) 447–454, http://dx.doi.org/10.1038/hr.2015.30.
[25] S. Peng, Y. Yu, K. Hao, H. Xing, D. Li, C. Chen, A. Huang, X. Hong, Y. Feng, Y. Zhang, J. Li, B. Wang, D. Wu, X. Wang, X. Xu, Heart rate-corrected QT interval is significantly associated with the blood pressure in chinese hypertensives, J. Electrocardiol. 39 (2) (2006) 206–210, http://dx.doi.org/10.1016/j.jelectrocard.2005.08.007.
[26] Michael A. Bauml, Donald A. underwood, Left Ventricular hypertrophy: an overlooked cardiovascular risk factor, Cleve. Clin. J. Med. 77 (6) (2010) 381–387, http://dx.doi.org/10.3949/ccjm.77a.09158.
[27] L.M. Ruilope, R.E. Schmieder, Left Ventricular hypertrophy and clinical outcomes in hypertensive patients, Am. J. Hypertens. 21 (5) (2008) 500–508, http://dx.doi.org/10.1038/ajh.2008.16.
[28] A.L. Goldberger, L.A. Amaral, L. Glass, J.M. Hausdorff, P.C. Ivanov, R.G. Mark, J.E. Mietus, G.B. Moody, C.-K. Peng, H.E. Stanley, Physiobank, physiotoolkit, and physionet: components of a new research resource for complex physiologic signals, Circulation 101 (23) (2000) e215–e220.
[29] M. Kachuee, M.M. Kiani, H. Mohammadzade, M. Shabany, Cuff-less High-accuracy calibration-free blood pressure estimation using pulse transit time, IEEE International Symposium on Circuits and Systems (ISCAS'15) (2015).
[30] X.R. Ding, Y.T. Zhang, Photoplethysmogram intensity ratio: a potential indicator for improving the accuracy of PTT based cuffless, Blood Pressure Estimation IEEE 37th Annu Int Conf Eng Med Biol Soc Milan Italy (2015), http://dx.doi.org/10.1109/EMBC.2015.7318383.
[31] H. Njoum, P. Kyriacou, A photoplethysmography for the assessment of haemorheology, Sci. Rep. 7 (2017).
[32] C.C. Wei, An Innovative method to measure the Peripheral Arterial Elasticity: spring constant modelling based on the arterial pressure wave with radial vibration, Ann. Biomed. Eng. 39 (11) (2011) 2695–2705, http://dx.doi.org/10.1007/s10439-011-0357-7.
[33] Yuh-Ying Lin Wang, C.C. Chang, J.C. Chen, H. Hsiu, W.K. Wang, Pressue wave propagation ino arteries A model with radial dilatation for simulating the behaviour of a real artery, IEEE Eng. Med. Biol. Mag. 16 (1) (1997), http://dx.doi.org/10.1109/51.566153.
[34] F.M. White, Fluid Mechanics, Mass: WCB/McGraw-Hill, Boston, 1999.
[35] Frank M. White, Isla Corfield, Viscous Fluid Flow, vol. 3, McGraw-Hill, New York, 2006.
[36] Arturo Evangelista, Frank A. Flachskampf, Raimund Erbel, Francesco Antonini-Canterin, Charalambos Vlachopoulos, Guido Rocchi, Rosa Sicari, Petros Nihoyannopoulos, Jose Zamorano, on behalf of the European Association of Echocardiography, Echocardiography in aortic diseases: EAE recommendations for clinical practice, Eur. J. Echocardiogr. 11 (2010) 645–658, http://dx.doi.org/10.1093/ejechocard/jeq056.
[37] W.E. Brant, The Core Curriculum: Ultrasound. Philadelphia, Williams & Wilkins, Lippincott, 2001.
[38] S. Satpathy, S. Satpathy, P.K. Nayak, Correlation of blood pressure and QT interval, J. Physiol. Pharm. Pharmacol. (2017), http://dx.doi.org/10.5455/njppp.2018.8.0934414092017.
[39] A.A. Fossa, T. Wisialowski, K. Crimin, E. Wolfgang, J.P. Couderc, M. Hinterseer, S. Kaab, W. Zareba, F. Badilini, N. Sarapa, Analyses of dynamic beat-to-beat

QT-TQ interval (ECG restitution) changes in humans under normal sinus rhythm and prior to an event of torsades de pointes during QT prolongation caused by sotalol, Ann. Noninvasive Electrocardiol. 12 (4) (2007) 338–348, http://dx.doi.org/10.1111/j.1542-474X.2007.00183.x.

[40] M.H. Imam, C.K. karmakar, H.F. Jelinek, M. Palaniswami, A.H. Khandoker, Analyzing systolic diastolic interval interaction characteristics in Diabetic Cardiac autonomic neuropathy progression, IEEE J. Transl. Eng. Health Med. 3 (2015), http://dx.doi.org/10.1109/JTEHM.2015.2462339.

[41] M. Awad, R. Khanna, Efficient Learning Machines, Springer, Berkeley C.A, 2015, pp. 67–80, Ch. Support Vector Regression.

[42] K. Bartels, R.H. Thiele, Advances in photoplethysmography: beyond arterial oxygen saturation, J. Can. Anesth. 62 (2015) 1313–1328, http://dx.doi.org/10.1007/s12630-015-0458-0.

[43] A. Vakily, H. Parsaei, M.M. Movahhedi, M.A. Sahmeddini, A system for continuous estimating and monitoring cardiac output via arterial waveform analysis, J Biomed Phys. Eng. 7 (2) (2017) 181–190.

[44] Adriana Arza Valdés, Jesús Lázaro, Eduardo Gil, Pablo Laguna, Jordi Aguiló, Raquel Bailón, Pulse transit time and pulse width as potential measure for estimating beat-to-beat systolic and diastolic blood pressure, Comput. Cardiol. (2013) 887–890.

[45] Ian B. Wilkinson, Helen MacCallum, Laura Flint, John R. Cockcroft, David E. Newby, David J. Webb, The influence of HR on augmentation index and central arterial blood pressure in humans, J. Physiol. 525 (2000) 263–270, http://dx.doi.org/10.1111/j.1469-7793.2000.t01-1-00263.x.

[46] D. Sparrow, H.E. Thomas Jr., B. Rosner, S.T. Weiss, The realationship of baseline ECG to blood pressure change, JAMA 250 (10) (1983) 1285–1288, http://dx.doi.org/10.1001/jama.1983.03340100019021.

[47] G.Z. Sun, Y. Zhou, N. Ye, S.J. Wu, Y.X. Sun, Independent influence of blood pressure on QTc interval: results from a Chinese population, Biomed Res. Int. (2019), http://dx.doi.org/10.1155/2019/1656123.